Magic Angle Spinning NMR of Paramagnetic Proteins

MICHAEL J. KNIGHT,[†] ISABELLA C. FELLI,[‡]
ROBERTA PIERATTELLI,[*,‡] LYNDON EMSLEY,[†] AND
GUIDO PINTACUDA[*,†]

[†]Université de Lyon, Institut de Sciences Analytiques (CNRS/ENS-Lyon/UCB Lyon 1),
Centre de RMN à Très Hauts Champs, 5 rue de la Doua, 69100 Villeurbanne, France,
and [‡]Department of Chemistry "Ugo Schiff" and Magnetic Resonance Center
(CERM), University of Florence, via Luigi Sacconi 6 — 50019 Sesto Fiorentino, FI, Italy

RECEIVED ON DECEMBER 24, 2012

CONSPECTUS
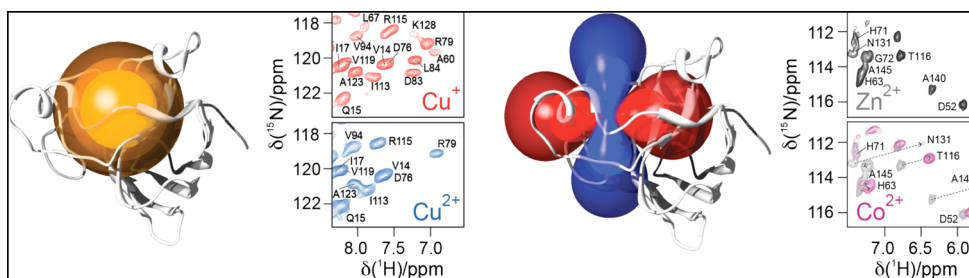
Metal ions are ubiquitous in biochemical and cellular processes. Since many metal ions are paramagnetic due to the presence of unpaired electrons, paramagnetic molecules are an important class of targets for research in structural biology and related fields. Today, NMR spectroscopy plays a central role in the investigation of the structure and chemical properties of paramagnetic metalloproteins, linking the observed paramagnetic phenomena directly to electronic and molecular structure.

A major step forward in the study of proteins by solid-state NMR came with the advent of ultrafast magic angle spinning (MAS) and the ability to use ^{1}H detection. Combined, these techniques have allowed investigators to observe nuclei that previously were invisible in highly paramagnetic metalloproteins. In addition, these techniques have enabled quantitative site-specific measurement of a variety of long-range paramagnetic effects. Instead of limiting solid-state NMR studies of biological systems, paramagnetism provides an information-rich phenomenon that can be exploited in these studies.

This Account emphasizes state-of-the-art methods and applications of solid-state NMR in paramagnetic systems in biological chemistry. In particular, we discuss the use of ultrafast MAS and [1]H-detection in perdeuterated paramagnetic metalloproteins. Current methodology allows us to determine the structure and dynamics of metalloenzymes, and, as an example, we describe solid-state NMR studies of microcrystalline superoxide dismutase, a 32 kDa dimer. Data were acquired with remarkably short times, and these experiments required only a few milligrams of sample.

Introduction

Metal ions are ubiquitous in biochemical and cellular processes, and many of them are paramagnetic due to the presence of unpaired electrons.[1,2] Paramagnetic effects can be directly linked to electronic and molecular structure, and their measurement by NMR plays today a central role in the determination of structure and chemical properties of metalloproteins,[3−5] or of biomolecules modified with spin-labels.[6,7]

Following the introduction of suitable sample preparation schemes[8,9] and the determination of the first protein structure,[10] solid-state NMR spectroscopy has tremendously progressed to become a powerful tool for the structural and dynamical characterization of a variety of biological materials, ranging from microcrystalline samples to fibrils and membrane-associated systems,[11,12] but only a few high-resolution studies have been performed on paramagnetic metalloproteins. This is because a number of competing effects make the detection of signals close to a paramagnetic center difficult.

A key step forward was represented by the complete assignment of the ^{13}C,[15]N resonances of microcrystalline
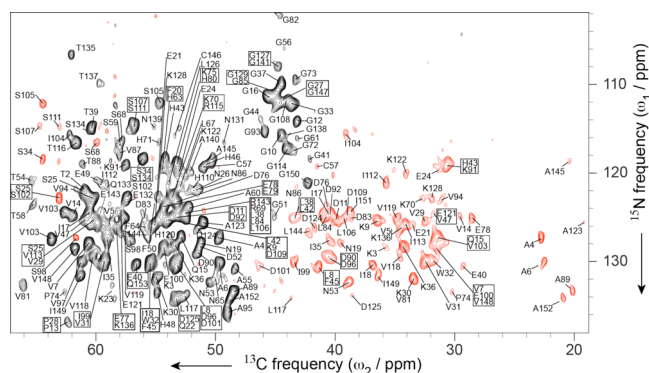
FIGURE 1. Assigned NCACB spectrum of Cu^{2+},Zn-SOD. Reproduced with permission from ref 13.

human Cu^{2+}, Zn-SOD in 2007,[13] where nuclei as close as 5 Å to the Cu^{2+} ion were observed. This work capitalized on the fact that solid-state NMR is routinely applied to the detection of low-γ nuclei, which are less susceptible to paramagnetic broadening than ^{1}H. Also, efficient dipolar-based polarization transfers can be used for cross-polarization and for homonuclear correlation experiments, as illustrated in Figure 1.

A breakthrough for high resolution NMR of paramagnetic systems came with the use of very fast (>30 kHz) MAS probes,[14,15] which brought a transformational change in sensitivity, enabling the detection of previously unobservable nuclei in highly paramagnetic materials. These techniques have subsequently been used on highly paramagnetic proteins, significantly reducing the "blind sphere" of resonances broadened beyond detection belonging to spins close to the metal center, and providing a powerful source of structural constraints for protein structure determination. This Account aims to cover these developments with the objective of demonstrating that paramagnetism needs no longer to be considered a limitation in solid-state NMR studies of biological systems, but on the contrary is an information-rich feature that should be routinely exploited.

Paramagnetic Effects

Paramagnetism manifests itself through enhanced relaxation (paramagnetic relaxation enhancement or "PRE"), altered shift anisotropy, and paramagnetic shifts (contact or "pseudocontact" shifts, PCS). These effects act over relatively long distances comparable to the size of protein domains, and have a well-defined dependence on the nuclear positions with respect to the paramagnetic ion or radical. These effects are sketched in Figure 2.

Paramagnetic Relaxation Enhancement (PRE). PRE denotes the increase in nuclear relaxation rate induced by random variations of the dipolar coupling between the
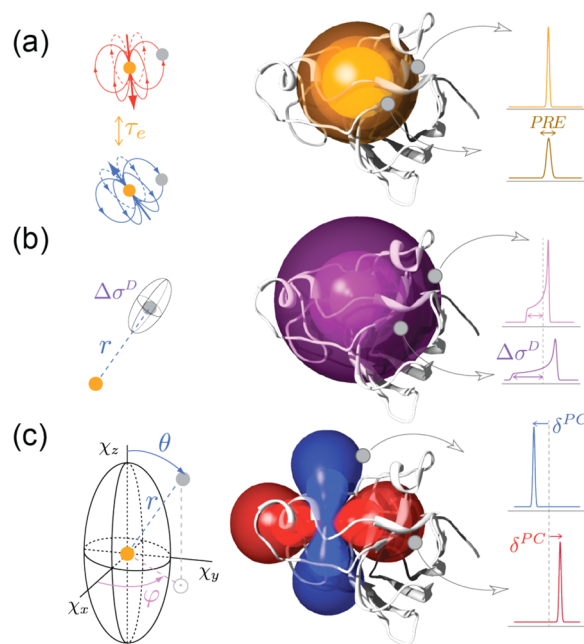

FIGURE 2. Spatial dependence of the paramagnetic relaxation enhancements (PRE) (a) of the dipolar shift anisotropy ($\Delta\sigma$) (b) and of the pseudocontact shift in the magnetic susceptibility principal axis system (δPC) (c). Isosurfaces depicting the three effects induced by Cu^{2+} or Co^{2+} paramagnetic centers are plotted on a ribbon representation of the crystal structure of SOD. Orange surfaces represent isosurfaces of PREs, isosurfaces of $\Delta\sigma$ are represented in violet, and blue and red surfaces represent respectively positive and negative isosurfaces of PCSs.

nuclear and the electronic moments. In solids, these fluctuations are mainly determined by electron relaxation (Figure 2a), which occurs with a typical correlation time τ_e usually in the range 10^{-7}–10^{-13} s, and they increase nuclear longitudinal and transverse relaxation rates R_1 ($=T_1^{-1}$) and R_2 ($=T_2^{-1}$) of surrounding nuclei according to the so-called Solomon equations:[16]

$$R_1^S = 2k\frac{\gamma_I^2 S(S+1)}{r^6}\left(\frac{\tau_e}{1+(\omega_I-\omega_S)^2\tau_e^2} + \frac{3\tau_e}{1+\omega_I^2\tau_e^2}\right.$$
$$\left. + \frac{6\tau_e}{1+(\omega_I+\omega_S)^2\tau_e^2}\right) \quad (1)$$

$$R_2^S = k\frac{\gamma_I^2 S(S+1)}{r^6}\left(4\tau_e + \frac{\tau_e}{1+(\omega_I-\omega_S)^2\tau_e^2}\right.$$
$$\left. + \frac{3\tau_e}{1+\omega_I^2\tau_e^2} + \frac{6\tau_e}{1+(\omega_I+\omega_S)^2\tau_e^2} + \frac{6\tau_e}{1+\omega_S^2\tau_e^2}\right) \quad (2)$$

where γ_I is the nuclear gyromagnetic ratio, S is the electron spin, r is the electron–nucleus distance, ω_I and ω_S are the nuclear and electronic Larmor frequencies respectively, τ_e is the electronic correlation time and the

constant $k = 1/15(\mu_0/4\pi)^2\hbar^2 g_e^2\mu_B^2$, in which μ_0 is the free space permittivity, $\hbar$ is Planck's constant divided by 2π, g_e is the free electron g-factor, and μ_B is the Bohr electron magneton.

Paramagnetic Shift Anisotropy. In the presence of a hyperfine interaction with an unpaired electron of spin S, Zeeman eigenstates for nuclear spin I are split into $2S+1$ levels. These splittings are never observed in a NMR experiment; because of the fast electronic relaxation rates, the nuclei see the electron spin only as a static magnetic moment averaged over the different Zeeman states, known as the Curie spin. A theoretical framework for treating the effects of the Curie spin upon the NMR spectrum is provided by the magnetic susceptibility χ_{iso}, which is the average magnetic dipole $\langle \mu_S \rangle$ of the electronic spin in the magnetic field B_0. In the high-temperature approximation, the expression of the average magnetic susceptibility per molecule (Curie law) is:[16]

$$\chi_{iso} = \mu_0 \frac{\langle \mu_S \rangle}{B_0} = \mu_0 \frac{g_e^2 \mu_B^2 S(S+1)}{3k_B T} \tag{3}$$

where k_B is Boltzmann's constant and T is the temperature. The Curie spin of the electron couples to the surrounding nuclei, which as a result experience a shielding $\Delta\sigma$. This "dipolar shift anisotropy" is equivalent to a traceless diamagnetic chemical shift anisotropy, but with a second-rank orientational dependence and an inverse third power distance dependence:

$$\Delta\sigma = \frac{\chi_{iso}}{\hbar\gamma_I r^3} = \frac{\mu_0}{\hbar\gamma_I r^3} \frac{g_e^2 \mu_B^2 S(S+1)}{3k_B T} \tag{4}$$

In a static powder sample, all possible crystallite orientations are present simultaneously, and the spectrum is the result of a sum over all orientations, leading to the "powder pattern" line shape. This effect is illustrated in Figure 2b, which shows the typical line shape of a powder pattern corresponding to the shift anisotropy, as well as surfaces of constant $\Delta\sigma$ around a metal center.

Pseudocontact Shift. In many cases, χ is a tensor, as occurs if the system is orbitally degenerate, if there is a zero-field splitting or if there is strong spin−orbit coupling. In such cases, the average electronic magnetic moment is dependent on the orientation of the system relative to the applied magnetic field. In general, therefore, χ has rank-0 and rank-2 components. In its principal axis system (PAS), χ can be defined by its isotropic value χ_{iso} and by its axial and rhombic anisotropies $\Delta\chi_{ax}$ and $\Delta\chi_{rh}$:

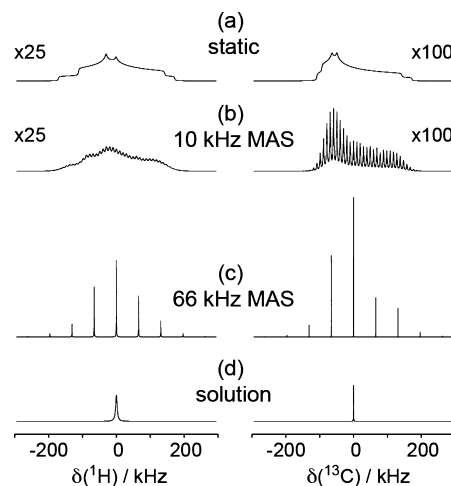$$\Delta\chi_{ax} = \chi_{zz} - \frac{\chi_{xx} + \chi_{yy}}{2} \tag{5}$$

FIGURE 3. Simulated ^{1}H (left) and ^{13}C (right) NMR spectra for a ^{1}H−^{13}C spin pair at 5 Å from a paramagnetic ion ($S = 3/2$, $\tau_e = 10^{-11}$s) in a metalloprotein. (a) Static; (b) 10 kHz MAS; (c) 66 kHz MAS; (d) solution.

$$\Delta\chi_{rh} = \chi_{xx} - \chi_{yy} \tag{6}$$

This rank-0 component is the pseudocontact shift (PCS or δ^{PC}),[16] which in the PAS of the susceptibility tensor is given by

$$\delta^{PC} = \frac{1}{12\pi r^3}\left\{ \Delta\chi_{ax}(3\cos^2\vartheta - 1) + \frac{3}{2}\Delta\chi_{rh}\sin^2\vartheta\cos 2\varphi \right\} \tag{7}$$

Here, ϑ and φ are the polar angles connecting the electron−nucleus vector to the PAS of the susceptibility tensor and r is the electron−nucleus distance. The spatial dependence of the PCS is represented in Figure 2c. Although this derivation makes use of the assumption that the paramagnetic center is point-localized, the majority of nuclei for which PCS are observable are beyond reach of significant electron delocalization from the paramagnetic center, so it is normally a safe assumption. In proteins, more complex treatments for the PCS dependence appear to become necessary only when nuclei directly coordinating the paramagnetic center are considered.[17]

Magic Angle Spinning

As illustrated in Figure 3, if magic angle spinning (MAS) is applied but at a frequency less than the size of the shift anisotropy, then the second-rank paramagnetic interactions are not completely averaged and the resulting spectrum comprises a set of sharp spinning sidebands separated by the MAS frequency. By contrast, when the spinning rate ω_r

exceeds the magnitude of these anisotropic interactions, complete coherent averaging is accomplished and only the frequencies of the isotropic interactions are directly observed in the spectra.[18] Similarly, only isotropic frequencies are observed in solution due to averaging of anisotropic interactions, but by incoherent motions. This results in an additional contribution to the PRE in solution (i.e., the so-called Curie mechanism), which is absent in solids since it is governed by fast rotational diffusion. Indeed it has been shown that the intrinsic linewidths in large paramagnetic compounds in the solid-state can actually be narrower than the solution equivalent.[19]

Overall, for paramagnetic solids, we can distinguish three regimes. In static samples (Figure 3a), broadening renders proton and carbon spectra unobservable.

Under moderate (<25 kHz) MAS (Figure 3b), the ^1H lines are not significantly narrowed, and ^{13}C (or ^{15}N) spectra split into numerous sidebands, which can be observed under favorable circumstances, but their linewidths are generally large due to the difficulty to decouple the strong time-dependent ^1H couplings. A remarkable increase in resolution, in sensitivity, and in coherence lifetimes T_2' of both ^{13}C and ^1H spins sets in at spinning rates larger than about 25 kHz (Figure 3c).[14,15,19,20] This effect becomes progressively more pronounced as spinning speeds increase toward the so-called ultrafast MAS regime (>50 kHz), in which the deleterious consequences of the large paramagnetic anisotropy are alleviated. More efficient refocusing of the homonuclear and heteronuclear dipolar couplings is obtained, and signals are concentrated into fewer sidebands. Additionally, in these conditions heteronuclear decoupling can be omitted without loss of resolution,[14,15] and ^1H linewidths are steeply reduced. These results become particularly striking when compared to the analogous behavior of a diamagnetic molecule given that the spectra of paramagnetic species may also be better resolved by virtue of their broad chemical shift range.

An example where ultrafast MAS has been applied to a paramagnetic protein is shown in Figure 4, demonstrating the case of CoMMP-12. Using 22 kHz MAS, work using ^{13}C detection was limited to the observation of nuclei located further than 9 Å from the Co^{2+} ion, with the difficulty in observing closer nuclear spins being attributed to increasingly large paramagnetic shift anisotropy effects in close proximity to the paramagnetic center. Ultrafast MAS at 60 kHz has enabled the detection of resonances in closer proximity to the Co^{2+} ion than before, up to 5.6 Å.[17]
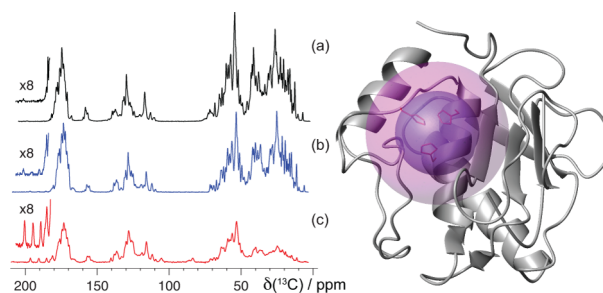

FIGURE 4. (a−c) ^{13}C NMR spectra of microcrystalline CoMMP-12 recorded (a) at 22 kHz MAS at 20 T (10k scans, 3 s interscan delay, total time = 15 h) and (b, c) at 60 kHz MAS at 21.2 T (15k scans, 2 s and 0.2 s interscan delay, respectively, total times = 15 h and 3h). (d) Regions of CoMMP-12 inaccessible by solid-state NMR at 22 kHz (outer sphere) and at 60 kHz (inner sphere). Reprinted with permission from ref 17.

Accelerated Acquisitions

Although PREs can be used to provide structural information due to their dependence upon the electron−nucleus distance (see below), a paramagnetic center also has the consequence of increasing the R_1 rate across the entire sample via a spin-diffusion mechanism, particularly for ^1Hs due to their relatively high gyromagnetic ratio. Since the recycle delay in an NMR experiment is predominantly governed by the recovery of ^1H magnetization, enhanced ^1H R_1 can be used to shorten the recycle delay and thereby allow more scans to be conducted per unit of time without loss of signal intensity due to saturation of the ^1H spins. Provided that sample heating is not an issue, the recycle delay under such conditions can be made very short.[14,15,20] This effect has long been exploited in NMR, but this becomes extremely pertinent in the case of solid proteins under ultrafast MAS, in which optimal ^{13}C and ^{15}N spectra can be obtained with low-power rf-fields during the whole experiment. As a result, recycle delays as short as a few tens of milliseconds can be used for detection of the paramagnetic signals, meaning experimental times for the acquisition of multidimensional correlations become correspondingly shorter.[21,22] Hence, when sidebands are sufficiently suppressed by very fast MAS, in combination with relaxation-enabled accelerated acquisition, the theoretical sensitivity of ^1H solid-state NMR for paramagnetic systems is greater than that for diamagnetic systems by an order of magnitude. This kind of sensitivity enhancement was extended to diamagnetic substrates using paramagnetic ion doping. This was achieved either by doping a protein crystal with Cu^{2+} complexed with EDTA,[23−25] or by incorporation of a thiol-specific EDTA-metal reagent bound to Cu^{2+} or Mn^{2+}.[26] The effect has been termed "paramagnetic-relaxation-assisted condensed data collection",[27] and it raises the possibility of

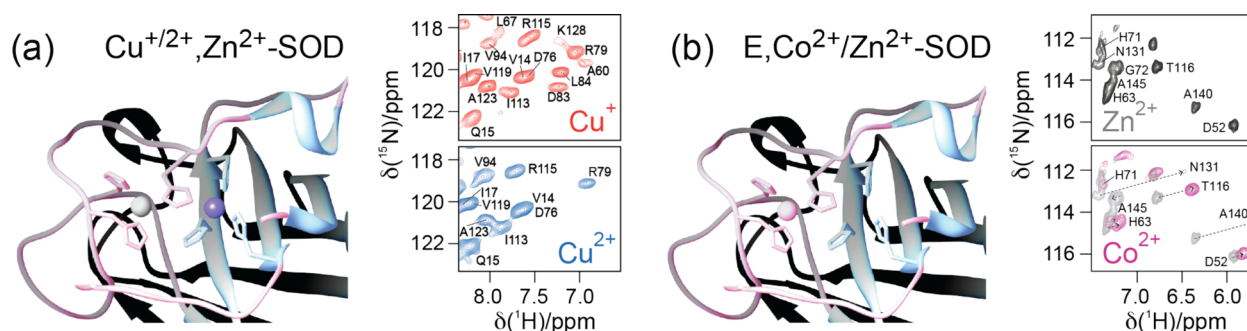**FIGURE 5.** (a) HSQCs from Cu^{2+},Zn-SOD and Cu$^+$,Zn-SOD. (b) HSQCs from Co^{2+}-SOD and Zn-SOD.[28,29]

applying fast MAS in combination with paramagnetic tagging or doping to systems which may be available only in small amounts, as for example in the case of Aβ(1−40) fibrils.

Fast-Relaxing and Slow-Relaxing Paramagnetic Centers

It is important to note that generally not all consequences of paramagnetism are manifest for a particular paramagnetic ion. The PREs are dependent upon the electronic correlation time of the particular paramagnetic ion, while PCS depend on the anisotropy of its χ tensor. The extent to which different ions cause paramagnetic effects is thus highly variable across the periodic table.

Figure 5 illustrates this phenomenon using the protein superoxide dismutase (SOD) as a benchmark. Human SOD[30] has the physiological function of protecting cells from oxidative stress by catalyzing the dismutation of the superoxide anion. The protein is a dimer, in which each 153-residue monomer has two high-affinity binding sites for metal cations. The metalation state can be experimentally controlled to obtain samples with different paramagnetic effects with minimal structural perturbation. In the most common physiological form, the two sites of each monomer are occupied by Cu and Zn, and the molecule cycles between the (paramagnetic) Cu^{2+} state and (diamagnetic) Cu$^+$ state during the reaction. The sample can be stably prepared with the oxidation state of the Cu ion in either the Cu$^+$ or Cu^{2+} form. Alternatively, a paramagnetic SOD sample and its diamagnetic analogue can be prepared in which one site is empty, and a (paramagnetic) Co^{2+} or a (diamagnetic) Zn^{2+} ion occupies the zinc site. In SOD, the Cu^{2+} ion has an electronic correlation time τ_e of 2.5×10^{-9} s which causes significant PRE effects (Figure 5a), but its susceptibility tensor is almost isotropic and thus does not produce sizable PCS (although it can cause significant contact shifts, the affected residues are often broadened beyond detection by PRE). On the other hand, ions such as Co^{2+} possess significant susceptibility anisotropy, and therefore cause significant PCS (Figure 5b). The correlation times for their electronic fluctuations τ_e are rapid (e.g., τ_e of Co^{2+} is in the range $1−10$ ps[16]), so due to absence of Curie relaxation in rigid solids, they enhance significantly the longitudinal relaxation of the surrounding spins, but have a negligible effect both on their observed linewidths and on the coherence lifetimes, and do not significantly reduce the efficiency of magnetization transfer. This is largely due to the R_2 PRE, induced by the Solomon mechanism alone, being small relative to nonparamagnetic contributions to transverse relaxation and coherence lifetime; the R_2 PRE is dominated by the zero-frequency spectral density as shown in eq 2. In these conditions, dipolar-based experiments optimized for the fast MAS regime (double quantum CP[22] or DREAM[31]) provide efficient ways to generate correlations between these nuclear spins, similarly to diamagnetic materials.

Perdeuteration and Fast MAS

The long-range nature of the PRE and PCS makes them powerful structural restraints, in particular where long-range information is difficult to obtain otherwise. However, the quantitative measurement of these effects in solids is often made very difficult by insufficient sensitivity when conventional heteronuclear detection methods are employed.

For example, site-specific PREs require the acquisition of long series of 2D correlation spectra to monitor relaxation decays, and in the solid state have been reported only for the model protein GB1 using paramagnetic tags attached to engineered cysteine residues.[26,32,33] Similarly, measurement of PCS with ^{13}C-detection had only been reported in pioneering studies.[34,35] The key limitations here were the relatively low resolution of 2D ^{13}C−^{13}C and ^{15}N−^{13}C maps, and the low sensitivity of ^{13}C-detected experiments with current technology.

In principle, these disadvantages could be overcome using direct acquisition of proton NMR spectra. However, despite the narrowing effects provided by very fast MAS, which enable fast acquisition of ^{13}C and ^{15}N spectra, with spinning speeds limited to 60 kHz today ^{1}H linewidths may still be too broad to yield fully resolved two-dimensional correlations in large fully protonated proteins. This may pose a problem in the efficient site-specific and quantitative measurement of paramagnetic effects along a protein chain.

Perdeuteration followed by partial reprotonation of the exchangeable sites was suggested as a method to obtain high-resolution ^{1}H NMR spectra in diamagnetic peptides and proteins under moderate MAS rates.[36,37] At higher MAS rates, high resolution can be achieved with fully reprotonated samples.[38,39] This latter approach leads to the acquisition of sensitive and resolved NMR spectra of medium-size proteins, which can be used as 2D fingerprints for the backbone resonance assignment and for the high-sensitivity detection of ^{1}H$-^1$H proximities.[39] In a paramagnetic sample, this provides an ideal platform for easy quantitative measurement of relaxation rates and shifts. All of the spectra shown in Figure 5 were obtained on perdeuterated, 100% H^N-reprotonated samples.

Structure Determination with PREs and PCS

In solids, the focus of attention is generally the R_1 PREs and $R_{1\rho}$ (the longitudinal rotating-frame relaxation rate constant under spin-lock conditions) due to the inherent difficulty in measuring R_2 rates accurately (on account of large contributions from coherent effects), and since the ^{1}H relaxation parameters have so far been generally difficult to determine. Note that while ^{15}N R_1s has been shown to be reliable when measured at moderate spinning speeds,[40] ^{13}C R_1s and ^{15}N $R_{1\rho}$ only become accurate when measured under ultrafast MAS.[41,42] At lower spinning speeds, these latter rates are polluted by contributions from coherent effects, such as spin-diffusion or dipolar broadening.

Using the methodology described above, by controlling the Cu oxidation state and using the Cu$^+$,Zn state as the diamagnetic reference, ^{15}N and ^{13}C R_1 PREs have been measured in Cu,Zn-SOD. By exploiting the high sensitivity of ^{1}H-detection, less than 4 mg (0.5 μmol) sample was sufficient (Figure 6).[39] In this study, measurement of relaxation rates was based on the ^{15}N$-^1$H CP-HSQC dipolar correlation module, combined with a ^{15}N inversion$-$recovery block (for ^{15}N R_1 measurement),[40,43] ^{15}N spin-lock (for ^{15}N $R_{1\rho}$ measurement),[42,44] or additional ^{13}C$-^{15}$N specific transfers and ^{13}C inversion$-$recovery (for ^{13}C R_1 measurement).[41]
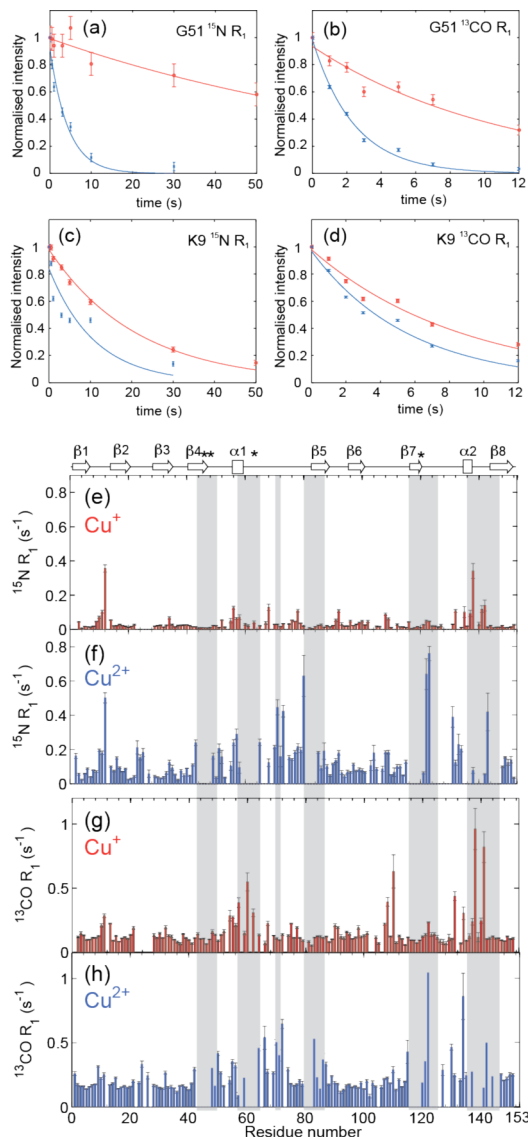

FIGURE 6. (a$-$d) Example ^{15}N and ^{13}C relaxation decays. (e,f) ^{15}N and (g,h) ^{13}C R_1 rates for Cu$^+$,Zn and Cu^{2+},Zn-SOD. Adapted with permission from ref 28.

This resulted in a powerful set of highly sensitive experiments, all based on the same "fingerprint" spectrum. Using these experiments, the enhancements in relaxation rates (Figure 6) were measured in human Cu,Zn-SOD as the difference between relaxation rate constants for SOD in its Cu^{2+} state and Cu$^+$ state, and provided more than one hundred PREs between 10 and 24 Å of the Cu ion. The study also reported ^{15}N $R_{1\rho}$ rates in diamagnetic and paramagnetic form, which were very similar, showing that the ^{15}N $R_{1\rho}$ can be used as a probe of dynamics even in paramagnetic systems.

Similarly, it was shown that the use of ^{1}H-detected solid-state correlations under ultrafast MAS on perdeuterated
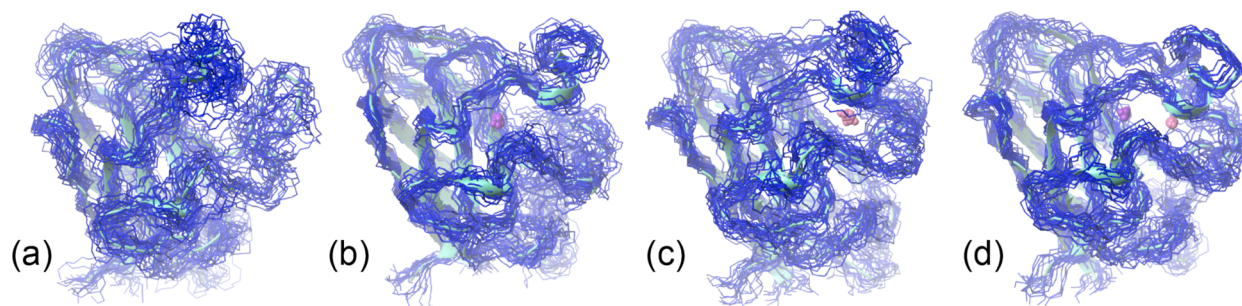
FIGURE 7. Solid-state NMR structure bundles for SOD, with different types of paramagnetic restraints: (a) no paramagnetic restraints, (b) with PREs, (c) with PCS, and (d) with both PCS and PREs. Pink is used to represent the Co ion, violet for the Cu ion, and the aquamarine ribbon diagram is the mean NMR structure for each case. Adapted from refs 28 and 29 (Copyright 2012 American Chemical Society).

substrates enables site-specific PCS to be measured, using Co^{2+}-SOD.[28] This study used 3D (H)CONH and (H)CANH correlations to obtain several hundred PCS, including ^1H PCS. In contrast to previous studies, PCS could be obtained for spins as close as 5 Å from the Co^{2+} ion. From these correlations, PCS were measured as the difference in chemical shifts relative to an isostructural diamagnetic analogue (here Zn-SOD), and their assignment was straightforward, exploiting the systematic change in chemical shifts along parallel lines in the spectra characteristic of PCS effects, as shown in Figure 5.

In order to use these data as structural restraints, PREs and PCS were incorporated into a structure determination protocol in combination with $^1H-^1H$ distance restraints measured from ^1H-detected 3D HHN$_{RFDR}$ experiments (totaling 297 $^1H-^1H$ pairs), chemical shift-derived dihedral angle restraints and ambiguous H-bond restraints using the program Cyana[45] in the Unio package.[46] In total, 85 ^{13}C and 90 ^{15}N quantitative PREs were used (converted into distance restraints using eqs 1 and 2), as well as 25 upper distance constraints from $^1H-^{15}N$ cross-peaks observable in the diamagnetic but not paramagnetic form.

In the case of PCS, prior to implementation as structure restraints it is necessary to determine the anisotropy of the susceptibility χ tensor, which is a function of the particular paramagnetic ion and the coordination environment imposed by the system. The χ-tensor requires the determination of eight parameters: the three position coordinates of the ion in the protein, the three Euler angles specifying the orientation of the PAS of the χ-tensor, and its two anisotropy parameters. With the availability of reference shifts and of an approximate structure model for a diamagnetic analogue, the determination of the χ anisotropy and its orientation, the assignment of PCS and their use as structural restraints was implemented as an iterative procedure.

As illustrated in Figure 7, for both PREs and PCS, the addition of these paramagnetic restraints significantly reduces the backbone RMSD of the resulting structure ensemble, taking it from 3.1 Å without any paramagnetic restraints down to 1.6 Å (PREs) or 1.7 Å (PCS). The simultaneous use of both effects from Cu,Zn-SOD and Co-SOD further improves the quality of the NMR structure, with a backbone RMSD which drops to 1.4 Å. In particular, the backbone geometry determined using all constraints (the bundle shown in Figure 7d) is extremely well-defined in the proximity of the Cu^{2+} and Co^{2+} binding sites.

It should be noted that, in some cases, depending on the metal ion used and the location of the binding site, neighbor effects need to be taken into consideration in solid studies, and methods exist to delineate the contributions of inter- and intramolecular effects for both PREs and PCS.[35,47] In principle, this can be used to determine crystalline packing.[48] In the cases of both Cu- and Co-SOD, due to the location of the binding sites, and to the low anisotropy found for the Co^{2+} χ tensor, neighbor effects were found to be negligible.

It is also possible to measure PREs using covalently bound paramagnetic tags. For example, Sengupta et al. demonstrated that ^{13}C and ^{15}N PREs induced by attaching a paramagnetic chelator to multiple cysteine mutants can be used in addition to dihedral angle restraints to determine the fold of GB1.[49] Due to the long-range nature of the PRE, and the fact that tags are necessarily attached to the surface of proteins, there is the possibility of intermolecular PRE effects. In the case of GB1, intermolecular PRE effects are relatively small and do not significantly affect PRE determination.

Paramagnetic Effects beyond Structure

Paramagnetic effects have also been used for a variety of purposes beyond structure calculation. For example, PRE effects have been used to examine the binding of Cu^{2+} to fibrils of the amyloidogenic peptide Aβ(1−40),[50] which has biological interest due to the elevated concentration of Cu^{2+} in cells containing amyloid plaques.

Another application of PREs in structural investigation by NMR is protein surface solvent accessibility, to which solid-state NMR has been applied in the case of microcrystalline SH3.[51] Here, a perdeuterated sample was used to limit $^1H-^1H$ spin diffusion, and the ^1H R_1 was measured site-specifically for amide protons of the protein backbone in a sample doped with Cu-EDTA. Regions exhibiting large PREs were found to be highly accessible to solvent, validating the method as a means of investigating solvent accessibility in the solid state. This raises interest since similar approaches have also been successful in solution-state NMR for the identification of interaction surfaces on proteins.

Conclusions

Given that metalloproteins are common in biochemistry and include important proteins with metal containing cofactors, the methods described above for structure investigation are potentially very broadly applicable to a wide range of systems which cannot be accessed by other atomic-resolution techniques, from membrane-embedded systems to fibrillar aggregates. These approaches can even be extended to otherwise diamagnetic proteins by the use of paramagnetic tagging. Extension of existing methods to the ^1H-detected schemes discussed above would undoubtedly make complex targets accessible. Additionally, the ^1H-detected methodology described above opens up many avenues beyond pure structure determination. For example, the possibility of detecting and assigning contact shift contributions for nuclear spins very close to the metal center in a solid sample[17] would be a uniquely powerful way to describe the complete electronic structure at the active site of a metalloprotein. Alternatively, the measurement of long-range paramagnetic effects with considerable precision lends itself as a probe for characterizing protein−protein or protein−drug interactions with considerable precision in solids.[52]

BIOGRAPHICAL INFORMATION

Dr. Michael J. Knight graduated in Biochemistry in 2006 at the University of Southampton, and received his Ph.D. in Biological NMR from the same University in 2009. Currently a postdoctoral fellow at the Ecole Normale Supérieure de Lyon, he works on the application and the development of solid-state NMR for studying the structure, dynamics and interactions of proteins.

Prof. Isabella C. Felli graduated with a degree in Chemistry in 1994 and obtained a Ph.D. in 1998 at the University of Florence with Prof. Bertini. She then worked with Prof. Bodenhausen in Tallahassee, and as an Alexander von Humboldt fellow with Prof. Griesinger in Frankfurt. Since 2005, she is an Associate Professor at the University of Florence. She is interested in the development of new methods for biomolecular NMR.

Prof. Roberta Pierattelli graduated in Chemistry at the University of Florence and received a Ph.D. in Chemistry at the same university in 1995. After a postdoctoral year at the University of Southampton, she was appointed as a Researcher at the University of Florence, where she became Associate Professor of Chemistry in 2002. Her research interests are mainly related to applications of NMR spectroscopy to the study of the structure and function of metalloproteins and their interactions.

Prof. Lyndon Emsley studied undergraduate chemistry at Imperial College and then obtained a Ph.D. in Lausanne with Prof. G. Bodenhausen in 1991. He was then a Miller Fellow in Berkeley, working with Prof. A. Pines from 1991 to 1993. Since 1994, he is a Professor of Chemistry at the Ecole Normale Supérieure de Lyon, where he develops new methods for the study of materials and molecules by NMR spectroscopy.

Dr. Guido Pintacuda studied Chemistry at the Scuola Normale Superiore in Pisa, where he graduated in 1997, and then completed his Ph.D. in 2000 with Prof. L. Di Bari and P. Salvadori. After working with Prof. G. Otting in Stockholm and Canberra, he moved to Lyon, where he is a CNRS Research Director (Full Professor) at the Ecole Normale Supérieure de Lyon. His current research concerns the development of new solid-state NMR methods for complex molecular systems in chemistry and biology, mostly with the help of paramagnetic metal ions.

REFERENCES

1 *Handbook on metalloproteins*; Bertini, I., Sigel, A., Sigel, H., Eds.; Marcel Dekker, Inc.: New York, 2001.

2 *Handbook of Metalloproteins*; Messerschmidt, A., Huber, R., Wieghardt, K., Poulos, T., Eds.; John Wiley & Sons: Chichester, 2001.

3 Banci, L.; Bertini, I.; Eltis, L. D.; Felli, I. C.; Kastrau, D. H.; Luchinat, C.; Piccioli, M.; Pierattelli, R.; Smith, M. The three-dimensional structure in solution of the paramagnetic high-potential iron-sulfur protein I from Ectothiorhodospira halophila through nuclear magnetic resonance. *Eur. J. Biochem.* **1994**, *225*, 715–725.

4 Bertini, I.; Luchinat, C.; Parigi, G.; Pierattelli, R. NMR spectroscopy of paramagnetic metalloproteins. *ChemBioChem* **2005**, *6*, 1536–1549.

5 Otting, G. Protein NMR using paramagnetic ions. *Annu. Rev. Biophys.* **2010**, *39*, 387–405.

6 Otting, G. Prospects for lanthanides in structural biology by NMR. *J. Biomol. NMR* **2008**, *42*, 1–9.

7 Keizers, P. M.; Ubbink, M. Paramagnetic tagging for protein structure and dynamics analysis. *Prog. NMR Spectrosc.* **2011**, *58*, 88–96.

8 McDermott, A.; Polenova, T.; Bockmann, A.; Zilm, K. W.; Paulson, E. K.; Martin, R. W.; Montelione, G. T. Partial NMR assignments for uniformly (^{13}C, ^{15}N)-enriched BPTI in the solid state. *J. Biomol. NMR* **2000**, *16*, 209–219.

9 Martin, R. W.; Zilm, K. W. Preparation of protein nanocrystals and their characterization by solid state NMR. *J. Magn. Reson.* **2003**, *165*, 162–174.

10 Castellani, F.; van Rossum, B.; Diehl, A.; Schubert, M.; Rehbein, K.; Oschkinat, H. Structure of a protein determined by solid-state magic-angle-spinning NMR spectroscopy. *Nature* **2002**, *420*, 98–102.

11 McDermott, A. E. Structure and dynamics of membrane proteins by magic angle spinning solid-state NMR. *Annu. Rev. Biophys.* **2009**, *38*, 385–403.

12 *NMR of Biomolecules: Towards Mechanistic Systems Biology*; Bertini, I., McGreevy, K. S., Parigi, G., Eds.; Wiley-VCH: Weinheim, 2012.

13 Pintacuda, G.; Giraud, N.; Pierattelli, R.; Böckmann, A.; Bertini, I.; Emsley, L. Solid-state NMR spectroscopy of a paramagnetic protein: assignment and study of human dimeric oxidized Cu^{II}-Zn^{II} superoxide dismutase (SOD). *Angew. Chem., Int. Ed.* **2007**, *46*, 1079–1082.

14 Ishii, Y.; Wickramasinghe, N. P.; Chimon, S. A new approach in 1D and 2D C-13 high-resolution solid-state NMR spectroscopy of paramagnetic organometallic complexes by very fast magic-angle spinning. *J. Am. Chem. Soc.* **2003**, *125*, 3438–3439.

15 Kervern, G.; Pintacuda, G.; Zhang, Y.; Oldfield, E.; Roukoss, C.; Kuntz, E.; Herdtweck, E.; Basset, J. M.; Cadars, S.; Lesage, A.; Coperet, C.; Emsley, L. Solid-state NMR of a paramagnetic DIAD-Fe-II catalyst: Sensitivity, resolution enhancement, and structure-based assignments. *J. Am. Chem. Soc.* **2006**, *128*, 13545–13552.

16 Bertini, I.; Luchinat, C.; Parigi, G. *Solution NMR of paramagnetic molecules: applications to metallobiomolecules and models*; Elsevier: Amsterdam, 2001; Vol. 2.

17 Bertini, I.; Emsley, L.; Lelli, M.; Luchinat, C.; Mao, J.; Pintacuda, G. Ultrafast MAS solid-state NMR permits extensive ^{13}C and ^{1}H detection in paramagnetic metalloproteins. *J. Am. Chem. Soc.* **2010**, *132*, 5558–5559.

18 Maricq, M. M.; Waugh, J. S. NMR kin rotating solids. *J. Chem. Phys.* **1979**, *70*, 3300–3316.

19 Kervern, G.; Steuernagel, S.; Engelke, F.; Pintacuda, G.; Emsley, L. Absence of curie relaxation in paramagnetic solids yields long H-1 coherence lifetimes. *J. Am. Chem. Soc.* **2007**, *129*, 14118–14119.

20 Wickramasinghe, N. P.; Shaibat, M.; Ishii, Y. Enhanced sensitivity and resolution in H-1 solid-state NMR spectroscopy of paramagnetic complexes under very fast magic angle spinning. *J. Am. Chem. Soc.* **2005**, *127*, 5796–5797.

21 Laage, S.; Marchetti, A.; Sein, J.; Pierattelli, R.; Sass, H. J.; Grzesiek, S.; Lesage, A.; Pintacuda, G.; Emsley, L. Band-selective ^{1}H-^{13}C cross-polarization in fast magic angle spinning solid-state NMR spectroscopy. *J. Am. Chem. Soc.* **2008**, *130*, 17216–17217.

22 Laage, S.; Sachleben, J. R.; Steuernagel, S.; Pierattelli, R.; Pintacuda, G.; Emsley, L. Fast acquisition of multi-dimensional spectra in solid-state NMR enabled by ultra-fast MAS. *J. Magn. Reson.* **2009**, *196*, 133–141.

23 Wickramasinghe, N. P.; Kotecha, M.; Samoson, A.; Past, J.; Ishii, Y. Sensitivity enhancement in ^{13}C solid-state NMR of protein microcrystals by use of paramagnetic metal ions for optimizing ^{1}H T$_1$ relaxation. *J. Magn. Reson.* **2007**, *184*, 350–356.

24 Linser, R.; Chevelkov, V.; Diehl, A.; Reif, B. Sensitivity enhancement using paramagnetic relaxation in MAS solid-state NMR of perdeuterated proteins. *J. Magn. Reson.* **2007**, *189*, 209–216.

25 Wickramasinghe, N. P.; Parthasarathy, S.; Jones, C. R.; Bhardwaj, C.; Long, F.; Kotecha, M.; Mehboob, S.; Fung, L. W.; Past, J.; Samoson, A.; Ishii, Y. Nanomole-scale protein solid-state NMR by breaking intrinsic ^{1}H T$_1$ boundaries. *Nat. Methods* **2009**, *6*, 215–218.

26 Nadaud, P. S.; Helmus, J. J.; Kall, S. L.; Jaroniec, C. P. Paramagnetic ions enable tuning of nuclear relaxation rates and provide long-range structural restraints in solid-state NMR of proteins. *J. Am. Chem. Soc.* **2009**, *131*, 8108–8120.

27 Nadaud, P. S.; Helmus, J. J.; Sengupta, I.; Jaroniec, C. P. Rapid acquisition of multidimensional solid-state NMR spectra of proteins facilitated by covalently bound paramagnetic tags. *J. Am. Chem. Soc.* **2010**, *132*, 9561–9563.

28 Knight, M. J.; Pell, A. J.; Bertini, I.; Felli, I. C.; Gonnelli, L.; Pierattelli, R.; Herrmann, T.; Emsley, L.; Pintacuda, G. Structure and backbone dynamics of a microcrystalline metalloprotein by solid-state NMR. *Proc. Natl. Acad. Sci. U.S.A.* **2012**, *109*, 11095–11100.

29 Knight, M. J.; Felli, I. C.; Pierattelli, R.; Bertini, I.; Herrmann, T.; Emsley, L.; Pintacuda, G. Rapid measurement of pseudocontact shifts in metalloproteins by proton-detected solid-state NMR spectroscopy. *J. Am. Chem. Soc.* **2012**, *134*, 14730–14733.

30 McCord, J. M.; Fridovich, I. Superoxide dismutase. An enzymic function for erythrocuprein (hemocuprein). *J. Biol. Chem.* **1969**, *244*, 6049–6055.

31 Verel, R.; Ernst, M.; Meier, B. H. Adiabatic dipolar recoupling in solid-state NMR: the DREAM scheme. *J. Magn. Reson.* **2001**, *150*, 81–99.

32 Nadaud, P. S.; Helmus, J. J.; Hofer, N.; Jaroniec, C. P. Long-range structural restraints in spin-labeled proteins probed by solid-state nuclear magnetic resonance spectroscopy. *J. Am. Chem. Soc.* **2007**, *129*, 7502–7503.

33 Nadaud, P. S.; Helmus, J. J.; Jaroniec, C. P. ^{13}C and ^{15}N chemical shift assignments and secondary structure of the B3 immunoglobulin-binding domain of streptococcal protein G by magic-angle spinning solid-state NMR spectroscopy. *Biomol. NMR Assignments* **2007**, *1*, 117–120.

34 Balayssac, S.; Bertini, I.; Lelli, M.; Luchinat, C.; Maletta, M. Paramagnetic ions provide structural restraints in solid-state NMR of proteins. *J. Am. Chem. Soc.* **2007**, *129*, 2218–2219.

35 Balayssac, S.; Bertini, I.; Bhaumik, A.; Lelli, M.; Luchinat, C. Paramagnetic shifts in solid-state NMR of proteins to elicit structural information. *Proc. Natl. Acad. Sci. U.S.A.* **2008**, *105*, 17284–17289.

36 Reif, B.; Jaroniec, C. P.; Rienstra, C. M.; Hohwy, M.; Griffin, R. G. ^{1}H-^{1}H MAS correlation spectroscopy and distance measurements in a deuterated peptide. *J. Magn. Reson.* **2001**, *151*, 320–327.

37 Chevelkov, V.; Rehbein, K.; Diehl, A.; Reif, B. Ultrahigh resolution in proton solid-state NMR spectroscopy at high levels of deuteration. *Angew. Chem., Int. Ed.* **2006**, *45*, 3878–3881.

38 Lewandowski, J. R.; Dumez, J. N.; Akbey, U.; Lange, S.; Emsley, L.; Oschkinat, H. Enhanced resolution and coherence lifetimes in the solid-state NMR spectroscopy of perdeuterated proteins under ultrafast magic-angle spinning. *J. Phys. Chem. Lett.* **2011**, *2*, 2205–2211.

39 Knight, M. J.; Webber, A. L.; Pell, A. J.; Guerry, P.; Barbet-Massin, E.; Bertini, I.; Felli, I. C.; Gonnelli, L.; Pierattelli, R.; Emsley, L.; Lesage, A.; Herrmann, T.; Pintacuda, G. Fast resonance assignment and fold determination of human superoxide dismutase by high-resolution proton-detected solid-state MAS NMR spectroscopy. *Angew. Chem., Int. Ed.* **2011**, *50*, 11697–11701.

40 Giraud, N.; Blackledge, M.; Goldman, M.; Böckmann, A.; Lesage, A.; Penin, F.; Emsley, L. Quantitative analysis of backbone dynamics in a crystalline protein from nitrogen-15 spin-lattice relaxation. *J. Am. Chem. Soc.* **2005**, *127*, 18190–18201.

41 Lewandowski, J. R.; Sein, J.; Sass, H. J.; Grzesiek, S.; Blackledge, M.; Emsley, L. Measurement of site-specific ^{13}C spin-lattice relaxation in a crystalline protein. *J. Am. Chem. Soc.* **2010**, *132*, 8252–8254.

42 Lewandowski, J. R.; Sass, H. J.; Grzesiek, S.; Blackledge, M.; Emsley, L. Site-specific measurement of slow motions in proteins. *J. Am. Chem. Soc.* **2011**, *133*, 16762–16765.

43 Schanda, P.; Meier, B. H.; Ernst, M. Quantitative analysis of protein backbone dynamics in microcrystalline ubiquitin by solid-state NMR spectroscopy. *J. Am. Chem. Soc.* **2010**, *132*, 15957–15967.

44 Krushelnitsky, A.; Zinkevich, T.; Reichert, D.; Chevelkov, V.; Reif, B. Microsecond time scale mobility in a solid protein as studied by the ^{15}N R$_{1rho}$ site-specific NMR relaxation rates. *J. Am. Chem. Soc.* **2010**, *132*, 11850–11853.

45 Herrmann, T.; Güntert, P.; Wüthrich, K. Protein NMR structure determination with automated NOE-identification in the NOESY spectra using the new software ATNOS. *J. Biomol. NMR* **2002**, *24*, 171–189.

46 Volk, J.; Herrmann, T.; Wüthrich, K. Automated sequence-specific protein NMR assignment using the memetic algorithm MATCH. *J. Biomol. NMR* **2008**, *41*, 127–138.

47 Nadaud, P. S.; Sengupta, I.; Helmus, J. J.; Jaroniec, C. P. Evaluation of the influence of intermolecular electron-nucleus couplings and intrinsic metal binding sites on the measurement of ^{15}N longitudinal paramagnetic relaxation enhancements in proteins by solid-state NMR. *J. Biomol. NMR* **2011**, *51*, 293–302.

48 Luchinat, C.; Parigi, G.; Ravera, E.; Rinaldelli, M. Solid-state NMR crystallography through paramagnetic restraints. *J. Am. Chem. Soc.* **2012**, *134*, 5006–5009.

49 Sengupta, I.; Nadaud, P. S.; Helmus, J. J.; Schwieters, C. D.; Jaroniec, C. P. Protein fold determined by paramagnetic magic-angle spinning solid-state NMR spectroscopy. *Nat. Chem.* **2012**, *4*, 410–417.

50 Parthasarathy, S.; Long, F.; Miller, Y.; Xiao, Y.; McElheny, D.; Thurber, K.; Ma, B.; Nussinov, R.; Ishii, Y. Molecular-level examination of Cu^{2+} binding structure for amyloid fibrils of 40-residue Alzheimer's beta by solid-state NMR spectroscopy. *J. Am. Chem. Soc.* **2011**, *133*, 3390–3400.

51 Linser, R.; Fink, U.; Reif, B. Probing surface accessibility of proteins using paramagnetic relaxation in solid-state NMR spectroscopy. *J. Am. Chem. Soc.* **2009**, *131*, 13703–13708.

52 Jovanovic, T.; McDermott, A. E. Observation of ligand binding to cytochrome P450 BM-3 by means of solid-state NMR spectroscopy. *J. Am. Chem. Soc.* **2005**, *127*, 13816–13821.